Mem. S.A.It. Vol. 73, 23

Memorie della

The Chemo-Dynamical Evolution of Elliptical Galaxies: Pre-heating and AGN heating

Daisuke Kawata, and Brad K. Gibson

Centre for Astrophysics & Supercomputing, Swinburne University, Australia
e-mail: dkawata,bgibson@astro.swin.edu.au

Abstract. We study the chemodynamical evolution of elliptical galaxies and their X-ray and optical properties using high-resolution cosmological simulations. Our Tree N-body/SPH code includes a self-consistent treatment of radiative cooling, star formation, supernovae feedback, and chemical enrichment. We present a series of ΛCDM cosmological simulations which trace the spatial and temporal evolution of abundances of heavy elements in both the stellar and gas components of galaxies. A giant elliptical galaxy formed in one of the simulations is quantitatively compared with the observational data in both the X-ray and optical regime. We implement a treatment of both pre-heating and AGN heating in this simulation, and examine the effect of these processes on elliptical galaxy formation. We find that the adopted pre-heating ($T = 10^7$ K at $z = 4$) is not strong enough to explain the observed X-ray or optical properties. On the other hand, our AGN heating model in which the gas inflow induces the AGN heating is consistent with both the X-ray and optical properties.

Key words. galaxies: elliptical and lenticular, cD —galaxies: formation—galaxies: evolution —galaxies: stellar content

1. Introduction

Developments in both ground- and space-based observational facilities has made it possible for astronomers to understand detailed self-consistent optical, X-ray, and theoretical analyses of galaxy formation and evolution. For the case of elliptical galaxies, optical observations provide constraints on the properties of the stellar component, while X-ray observations constrain the physical conditions of the hot interstellar medium (ISM).

Kawata & Gibson (2003b) (KB03b) presented a first attempt to explain both the X-ray and optical properties of observed elliptical galaxies via the use of self-consistent cosmological simulations. Using a standard "recipe" for galaxy formation, they found that radiative cooling is important to interpret the observed X-ray luminosity (L_X), temperature (T_X), and metallicity ($[Fe/H]_X$) of the hot gas of elliptical galaxies. However, they also found a serious problem in that the cooled gas also leads to excessive star formation at low

Send offprint requests to: D. Kawata
Correspondence to: Mail #31, PO Box 218, Hawthorn, VIC, 3122, Australia

redshift, and therefore results in underlying galactic stellar populations which are too blue with respect to observations. Their study demonstrates that the cross-check over both X-ray and optical properties provides stronger constraints for the theoretical models (more so than anyone taken in isolation), and is essential for any successful scenario of elliptical galaxy formation and evolution.

KG03b suggested that a heating mechanism which was not included in their simulations would be required to suppress this enhanced cooling and consequent star formation. In this paper, we examine two such potential mechanisms: pre-heating and heating by an Active Galactic Nucleus (AGN). Previous analytical and numerical studies have shown that the pre-heating of gas at high redshift may help to explain the X-ray luminosity and temperature of the hot gas (e.g. Borgani et al. 2002), although the source of the pre-heating remains unclear. On the other hand, recent observations suggest that all elliptical galaxies have a central black hole (e.g. Ferrarese & Merritt 2000). One might expect therefore that once the cold gas falls into the central part of a galaxy, the AGN may become "active" and heat up the surrounding gas, and might be able to blow out the gas from the system via a radio jet. Once the gas accretion is halted by such AGN heating, the AGN itself loses its fuel "source" and goes back to a quiescent state, which allows the gas to cool again. This self-regulation cycle may be capable of suppressing star formation for a significant period of time, without changing the effect of radiative cooling, which is in turn required to consider the indication for the observed X-ray properties. Several earlier studies of the effect of AGN heating on the hot gas of elliptical galaxies can be seen in Binney & Tabor (1995); Brighenti & Mathews (2002); Brüggen & Kaiser (2002). Our current study examines the effect of pre-heating and AGN heating on the optical properties as well as the X-ray properties in the context of a more self-consistent treatment of cosmological evolution.

2. Methods

Our simulations were carried out using `GCD+`, our original galactic chemodynamical evolution code. Details of the code are presented in Kawata (1999) and Kawata & Gibson (2003a,b). In `GCD+`, the dynamics of collisionless dark matter and stars is calculated using a gravitational Tree N-body code, and the gas component is modeled using Smoothed Particle Hydrodynamics (SPH). We calculate radiative cooling, star formation, chemical enrichment, and supernovae (SNe) feedback, self-consistently, and take into account both Type Ia and Type II SNe. We assume that SNe feedback is released as thermal energy.

We have carried out a series of high-resolution simulations within a standard ΛCDM cosmology (Ω_0=0.3, Λ_0=0.7, $\Omega_{\rm b}$=0.019h^{-2}, h=0.7, and σ_8=0.9). Gas dynamics and star formation are included only within the relevant high-resolution region (∼12 Mpc at z=0); the surrounding low-resolution region (∼43 Mpc) contributes to the high-resolution region only through gravity. The mass of individual gas particles in the high-resolution region was 5.9×10^7 $M_\odot$. We identified an appropriate elliptical galaxy analog in the high-resolution region, which acts as the focus for this study. The total virial mass of this target galaxy is 2×10^{13} $M_\odot$, similar in size to that of NGC 4472, a bright elliptical galaxy in the Virgo Cluster. The target galaxy is relatively isolated, with only a few low-mass satellites remaining at z=0. This target galaxy is the same system discussed in KG03b. Fig. 1 of KG03b shows the morphological evolution of dark matter in the simulation volume, and the evolution of the stellar component of the target galaxy. The galaxy forms through conventional hierarchical clustering between redshifts z=3 and z=1; the morphology has not changed dramatically since z=1.

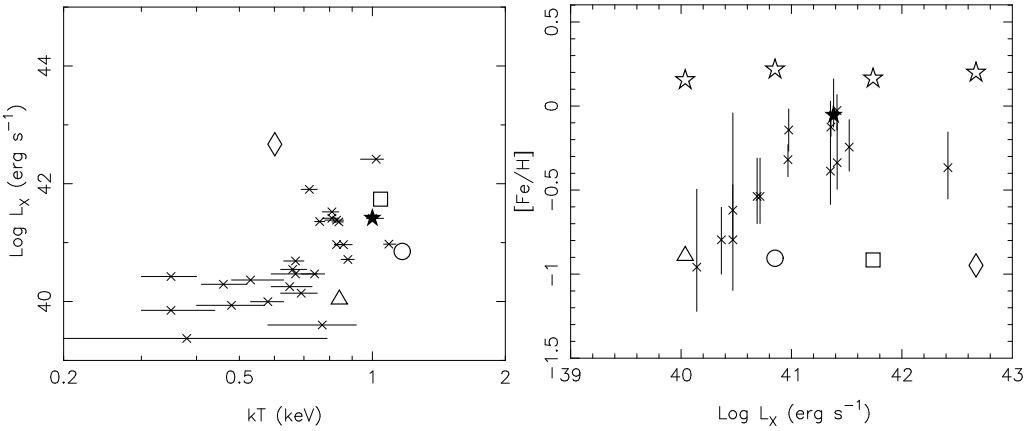

Fig. 1. Comparison of the simulated and observed (crosses with error bars) $L_X - T_X$ relations (*left panel*) and $[Fe/H]_X - L_X$ relations (*right panel*). The circle/square/diamond/triangle indicates the predictions of Model 1/2/3/4. Open stars in the right panel show the predicted mean metallicity of the stellar component for the four models. The observational data are from Matsushita, Ohashi, & Makishima (2000). The solid star presents the position of NGC 4472.

KG03b presented the results of three different radiative cooling and SNe feedback models. We use two of their models as reference models for this study; Model 1 here corresponds to Model B of KG03b, which includes cooling and weak feedback; Model 2 here corresponds to Model C of KG03b which mimics Model 1, but incorporates 100 times greater thermal energy (10^{52} erg) per supernova than Model 1. Since in this study we are interested in the effect of the pre-heating and the heating by AGN, we construct the additional two models:

Model 3: pre-heating model. The gas component in the entire simulation region is heated to a temperature of $T = 10^7$ K at redshift $z = 4$. Weak thermal SNe feedback (as in Model 1) is adopted.

Model 4: AGN heating model. The most bounded star particle in the target galaxy at $z = 1$ is assumed to be the heating source, i.e. the AGN "particle". Since the AGN heating requires gas fueling, we assume that the AGN heating is active only when the divergence of the velocity field of the surrounding gas of the AGN particle is negative, $\langle \nabla \cdot \boldsymbol{v} \rangle < 0$. The divergence of the velocity field of the neighbour gas particles is calculated using the SPH scheme. A constant thermal energy of 10^{44}erg s^{-1} is deposited to the neighbour gas particles when the above condition is satisfied. This energy is roughly consistent with observational estimates (e.g. Blanton, Sarazin & McNamara 2003). Strong thermal SNe feedback (as in Model 2) is also adopted.

For all the models, we examine both the resulting X-ray *and* optical properties, comparing them quantitatively with observation (see KG03b for details). The gas particles in our simulations carry with them knowledge of the density, temperature, and abundances of various heavy elements. Using the XSPEC `vmekal` plasma model, we derive the X-ray spectrum for each gas particle, and synthesize them within the assumed aperture (R$\sim$35 kpc). We next generate "fake" spectra with the response function of the XMM EPN detector, assuming an exposure time (40 ks) and target galaxy distance (17 Mpc). Finally, our XPSEC fitting provides the X-ray weighted temperatures and abundances of various el-

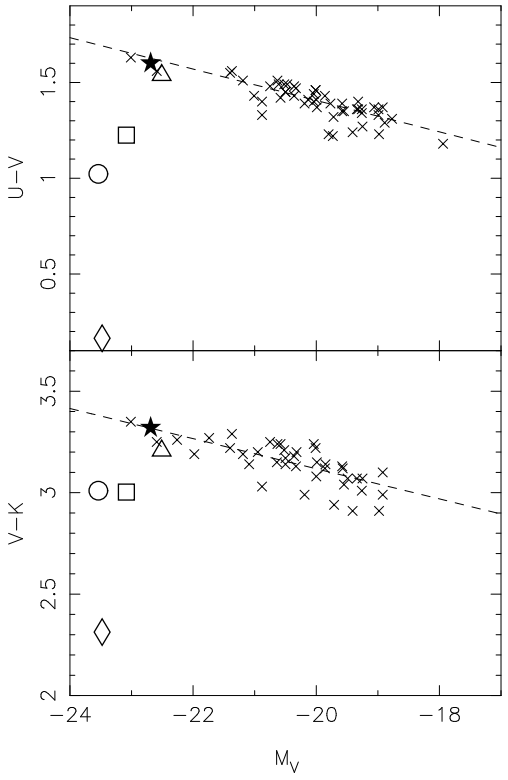

Fig. 2. Comparison of the simulated $U-V$ and $V-K$ CMRs (circle/square/diamond/triangle for Model 1/2/3/4) and those of the Coma cluster ellipticals (crosses). The observational data are from Bower, Lucey, & Ellis (1992). The dashed line shows the CMR fitted to the Coma Cluster galaxies. The solid star shows the position of NGC 4472.

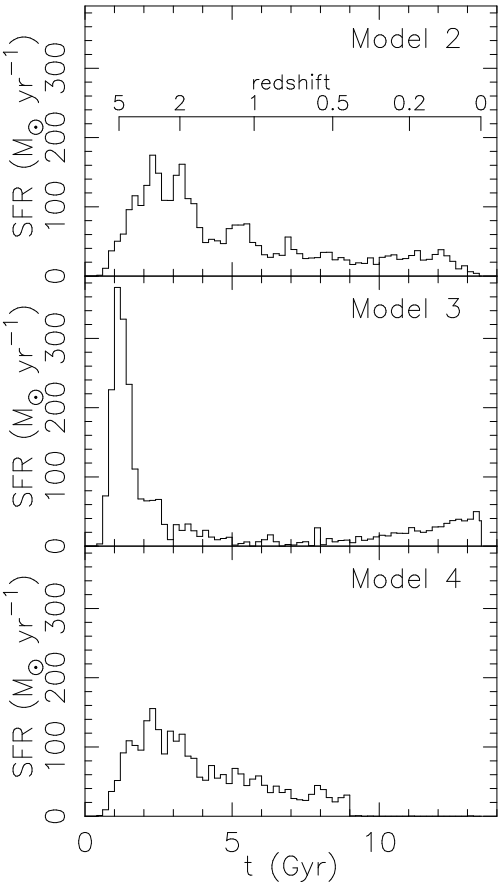

Fig. 3. Time variation of the star formation rate for Models 2 (upper), 3 (middle), and 4 (lower).

ements. Conversely, the simulated star particles each carry their own age and metallicity "tag", which enables us to generate an optical-to-near infrared spectral energy distribution for the target galaxy, when combined with our population synthesis code adopting simple stellar populations of Kodama & Arimoto (1997).

3. Results and Conclusion

To study both X-ray and optical properties, we examine the $L_X - T_X$ and $L_X - [Fe/H]_X$ relations for the X-ray properties, and the colour-magnitude relation (CMR) for the optical properties. Figs. 1 and 2 show the $L_X - T_X$ and $L_X - [Fe/H]_X$ relations and the CMRs for the four models, and compare the model results with the observational data. Models 1 and 2 are re-plot from Models B and C of KG03b. As shown in KG03b, current standard galaxy formation models, such as Models 1 and 2, can roughly reproduce the $L_X - T_X$ and $L_X - [Fe/H]_X$ relations. However, the optical colours of the resulting stellar components for these models are inconsistent with the observational data (Fig. 2), due to ex-

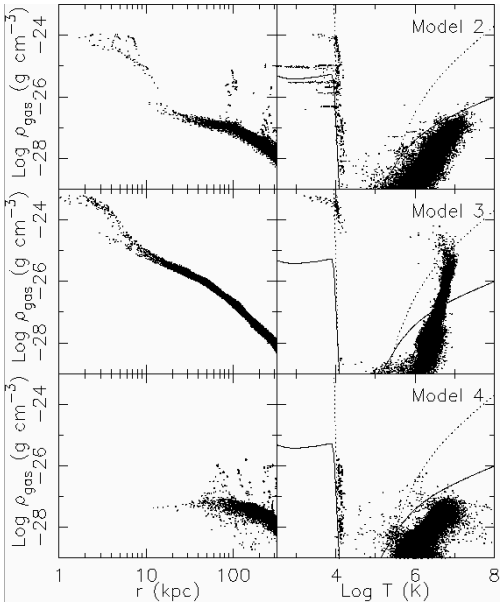

Fig. 4. Density vs radius (left) and density vs temperature (right) distributions of gas particles for Models 1 (upper), 2 (middle), and 3 (lower). The solid (dotted) curves separate the region where the cooling time is shorter (upper region) and longer than the Hubble (dynamical) time.

cessive star formation at low redshift (Fig. 3), which is induced by radiative cooling.

The pre-heating model, Model 3, leads to too high X-ray luminosity and too low temperature (Fig. 1). Fig. 4 shows that in Model 2 the gas whose cooling time, $t_{\rm cool}$, is shorter than the Hubble time, t_0, is changed into the cold gas. However, in Model 3 the gas whose $t_{\rm cool}$ is longer than the local dynamical time, $t_{\rm dyn} = (3\pi/16G\rho)^{1/2}$, can stay in the hot phase, which leads to the higher hot gas density, and thus the higher L_X. Also Fig. 3 shows that the pre-heating cannot suppress star formation until $z = 0$, although star formation is suppressed until $z \sim 0.5$ (see also Tornatore et al. 2003). Consequently, a larger amount of remaining gas leads to a higher star formation rate at $z = 0$, which results in a bluer colour than Models 1 and 2. This result demonstrates that the pre-heating we assumed here is not strong enough for this elliptical galaxy. A higher amount of the pre-heating will be examined in a future work (see also Borgani et al. 2002).

The most successful model is the AGN heating model, Model 4. Although the X-ray luminosity is slightly lower compared with the observed value of NGC 4472 (Fig. 1), Model 4 roughly reproduces both the X-ray and optical observational data. Fig. 4 shows that our AGN heating model gets rid of the cold gas in the central region, but does not change the hot gas profile significantly. As a result, the hot gas properties for Model 4 are similar to Model 2. This is due to the self-regulated AGN heating which guarantees that the hot gas is not "over-heated". We also found that, compared with Model 2, a larger fraction of iron ejected from stars is blown out from the system by the AGN heating, which results in a lower metallicity in the hot gas (Fig. 1). In addition, this AGN heating is powerful enough to stop the recent star formation, and leads to the observed red colours of elliptical galaxies (Fig. 2).

Our cosmological chemodynamical code makes it possible to undertake quantitative comparisons between numerical simulations and observational data in both the X-ray and optical regime with minimal assumptions. We find that the AGN heating induced by cold gas inflow can explain both the X-ray and optical observations of elliptical galaxies. Although our AGN model is rather simple and we focus on only one elliptical galaxy model, this result encourages more serious studies of the effect of the AGN heating on elliptical galaxy formation.

Acknowledgements. We acknowledge the financial support of the Australian Research Council and the Japan Society for the Promotion of Science through the Grants-in-Aid for Scientific Research (No. 14540221).

References

Binney J.J. & Tabor G. 1995, MNRAS 276, 663
Blanton E.L., Sarazin C.L., McNamara B.R. 2003, ApJ 585, 227
Bower, R.G., Lucey, J..R., & Ellis, R.S., 1992, MNRAS, 254, 589
Borgani S. et al. 2002, MNRAS 336, 409
Brighenti F. & Mathews W.G. 2002 ApJL, 574, L11
Brüggen M., Kaiser C.R. 2002, Nature 418, 301
Ferrarese, L. & Merritt, D., 2000, ApJL 539, 9
Kaiser N. 1991, ApJ 383, 104
Kawata D. 1999, PASJ 51, 931
Kawata D. & Gibson B.K. 2003a, MNRAS 340, 908
Kawata D. & Gibson B.K. 2003b, MNRAS 346, 135 (KG03b)
Kodama T. & Arimoto N. 1997 A&A, 320, 41
Matsushita, K., Ohashi, T., & Makishima, K., 2000, PASJ, 52, 685
Tornatore L. et al. 2003, MNRAS 342, 1025